

Growth of conformal single-walled carbon nanotube films from Mo/Fe/Al₂O₃ deposited by electron beam evaporation

Anastasios John Hart^{*}, Alexander H. Slocum, Laure Royer

*Precision Engineering Research Group, Department of Mechanical Engineering, Massachusetts Institute of Technology,
77 Massachusetts Avenue, Room 3-470, Cambridge, MA 02139, USA*

Received 7 April 2005; accepted 15 July 2005
Available online 26 August 2005

Abstract

We discuss growth of high-quality carbon nanotube (CNT) films on bare and microstructured silicon substrates by atmospheric pressure thermal chemical vapor deposition (CVD), from a Mo/Fe/Al₂O₃ catalyst film deposited by entirely electron beam evaporation. High-density films having a tangled morphology and a Raman G/D ratio of at least 20 are grown over a temperature range of 750–900 °C. H₂ is necessary for CNT growth from this catalyst in a CH₄ environment, and at 875 °C the highest yield is obtained from a mixture of 10%/90% H₂/CH₄. We demonstrate for the first time that physical deposition of the catalyst film enables growth of uniform and conformal CNT films on a variety of silicon microstructures, including vertical sidewalls fabricated by reactive ion etching and angled surfaces fabricated by anisotropic wet etching. Our results confirm that adding Mo to Fe promotes high-yield SWNT growth in H₂/CH₄; however, Mo/Fe/Al₂O₃ gives poor-quality multi-walled CNTs (MWNTs) in H₂/C₂H₄. An exceptional yield of vertically-aligned MWNTs grows from only Fe/Al₂O₃ in H₂/C₂H₄. These results emphasize the synergy between the catalyst and gas activity in determining the morphology, yield, and quality of CNTs grown by CVD, and enable direct growth of CNT films in micromachined systems for a variety of applications.

© 2005 Elsevier Ltd. All rights reserved.

Keywords: Carbon nanotubes; Chemical vapor deposition; Microstructure; Annealing; Oxidation; Raman spectroscopy

1. Introduction

While many prospective applications require control of the position and orientation of individual or groups of CNTs, there are also many applications for films of tangled CNTs as functional device elements such as thin-film transistors [1], chemical sensors [2], flow sensors [3], and electrical contacts [4]. These films may be grown directly on substrates and subsequently processed by lift-off patterning, functionalization, contact metal deposition, CVD deposition of structural layers, and other methods; alternatively the CNTs may be grown

in bulk and selectively deposited onto devices by wet chemical methods [5,6].

Synergy between the catalyst, carbon source, and growth conditions such as temperature and flow rate is vital for obtaining a high-yield of high-quality CNTs by chemical vapor deposition (CVD). The performance of a catalyst in nucleating and continuing the growth of CNTs depends on several factors in addition to its elemental composition, including the size and surface properties of the catalyst particles and the interactions between the catalyst and the support. The supporting layer can significantly promote or hinder CNT growth by the nature of its physical, chemical, and electronic interactions with the catalyst [7,8]. Especially effective material combinations for CNT growth include Al₂O₃-supported Mo/Fe with CH₄ [9], Ni or Co with C₂H₂

^{*} Corresponding author. Tel.: +1 617 258 8541; fax: +1 617 258 6427.

E-mail address: ajhart@mit.edu (A.J. Hart).

[10], and SiO₂-supported Mo/Co with CO [11] or alcohol [12].

The performance of a catalyst is also coupled to the deposition process, which can roughly be categorized as a physical method such as magnetron sputtering or e-beam evaporation, or a chemical method for preparing metal clusters in solution and subsequently depositing the clusters on a substrate. For sputtering deposition, Shin et al. demonstrated that the temperature and background pressure of the sputtering process, which affects the grain size and density of Ni thin films, is directly related to the length and diameter of vertically-aligned CNTs grown by thermal CVD of C₂H₂ [13]. In comparison, chemical methods [14,15,9] enable direct control of particle composition and particle size, which can give direct control of CNT diameters [16]. However, deposition methods for these solutions, including spin-coating [9,17], dip-coating [18], and contact printing [19,20], are less favorable than physical methods for uniformity over large areas, and for coating of microstructures. For example, with contact printing it is difficult to coat oblique features; with dip-coating the solution tends to collect and dry in recessed areas; and with spin-coating, surface tension effects oppose uniform coating of topography and non-uniformity is especially prevalent as solutions wick away from edges and corners of features. It is also straightforward to pattern physically-deposited metal films to micron-scale dimensions using liftoff of standard image-reversal photoresist in acetone, and therefore dictate uniform area-selective growth of CNTs on large substrates.

We present a parametric study of CNT growth from a Mo/Fe/Al₂O₃ catalyst deposited by e-beam evaporation, and demonstrate uniform and conformal growth of CNT films by atmospheric-pressure thermal CVD on a variety of microstructures. Presence of H₂ in addition to CH₄ is necessary for CNT growth, and dense films of high-quality SWNTs are grown over a wide range of conditions from a H₂/CH₄ mixture. Our experiments confirm that Mo promotes SWNT growth from CH₄, and indicate that Mo hinders MWNT growth from C₂H₄, while a Fe/Al₂O₃ film in C₂H₄ gives an exceptional yield of vertically-aligned MWNTs. This repeatable and versatile process for enhancing micromachined surfaces with uniform CNT films enable the robust integration of CNTs in micromachined devices.

2. Materials and methods

2.1. Catalyst film

A catalyst film of 20 nm Al₂O₃, 1.5 nm Fe, and 3 nm Mo is deposited by e-beam evaporation in a single pump-down cycle using a Temescal VES-2550, with a

FDC-8000 Film Deposition Controller. The substrates are plain (100) 6" silicon wafers (p-type, 1–10 Ω cm, Silicon Quest International), which have been cleaned using a standard "pirahna" (3:1 H₂SO₄:H₂O₂) solution. After catalyst deposition, no further cleaning or dedicated oxidation is necessary prior to nanotube growth. The Al₂O₃ is deposited by direct evaporation from a crucible of high-purity crystals, rather than by evaporation of Al with a slight background pressure of O₂ [21,22], or by other methods such as spin-coating of a sol-gel precursor [23]. While CNT growth from catalyst metals deposited on an Al layer has been reported [24,25], Al must be oxidized to prevent damage to the catalyst by formation of an Al-Si eutectic at 577 °C [26].

CNT growth from Mo/Fe catalysts is well-known, and addition of a small amount of Mo (as low as 20% [24]) to Fe significantly enhances catalytic activity for CNT growth. Furthermore, while Fe is a sufficient monometallic catalyst under a wide range of conditions, CNT growth from pure Mo (supported on Al₂O₃ particles) has been reported only in CO at 1200 °C [27]. Deng et al. suggested from simulations that certain bi-metallic catalysts give a higher CNT yield than monometallic catalysts because one metal (in the case of Mo/Fe, Mo) is responsible for nucleation, and the other metal is responsible for growth and defect repair [28]. However, considering much experimental evidence that Fe is necessary for nucleation and that an unfavorable ratio of Mo/Fe significantly affects yield, the complex interaction of Fe and Mo may not be divisible into primary behaviors. It has also been hypothesized that molybdenum carbide forms from Mo in a hydrocarbon environment, which causes aromatization of CH₄, which in turn improves nanotube growth from Fe [29,23].

Furthermore, compared to other supporting layers including TiN and TiO₂, Al₂O₃ is an especially effective supporting layer for Fe catalysts for CNT growth [30,23,31]. The performance of Al₂O₃ can be attributed to strong dispersion effects which limit agglomeration of Fe clusters on the Al₂O₃ surface [8], the nature of metal-support interactions in promoting electron transfer between the catalyst and the support [7], high surface roughness and porosity which improves the diffusion of reactant gases to the catalyst clusters [30,32], and enhanced decomposition of hydrocarbons on the Al₂O₃ surface [33,34]. Some reports indicate the crystallinity of the support material critically affects CNT growth, whereas others indicate that amorphous support materials are better supports. For example, Hongo et al. demonstrate that SWNT growth on Fe-coated Al₂O₃ is affected by both the film thickness and the crystallographic orientation of the substrate, which determines the interaction energy with Fe. On the other hand, Vander Wal et al. qualitatively show that fumed (amorphous) oxides give higher yield than powdered

crystalline oxides. In this study, the effect of crystallinity may be masked by the increased surface area allowing more uniform dispersion of the metal catalyst particles. Furthermore, the support layer should be sufficiently thick to prevent interdiffusion of the catalyst metal into the substrate. Therefore, while it has been demonstrated that the CNT growth is also highly sensitive to support layer thickness [35,36], relatively steady behavior should be observed beyond a certain thickness.

2.2. CVD procedure

CNT growth is performed in a conventional single-zone atmospheric pressure quartz tube furnace, with an inside diameter of 22 mm and a 30 cm long heating zone. Flows of argon (Ar, 99.999%, Airgas), methane (CH_4 , 99.995%, BOC), ethylene (C_2H_4 , 99.5%, Airgas), and hydrogen (H_2 , 99.999%, BOC) are metered using manual needle valve rotameters (Matheson Tri-Gas and Gilmont Instruments). The rotameters were purchased new and were calibrated. We estimate 1–2% relative accuracy and repeatability of the flow ratios, and 5% accuracy of the total flows.

After loading the sample in the tube, the furnace is flushed with 400 sccm Ar for 10 min to displace atmospheric air. Next, the furnace temperature is ramped linearly to the setpoint temperature, for 30 min, with a flow of 400 sccm Ar. The Ar flow is maintained for an additional 15 min while the furnace temperature stabilizes at the setpoint, and then the reactant gases are introduced for the growth period of typically 15 min. 400 sccm Ar is again introduced for 10 min to displace the growth gases from the tube and then the Argon flow is reduced to a trickle while the furnace cools.

2.3. CNT characterization

Scanning electron microscopy (SEM) of as-grown samples is performed using a Philips XL30 FEG-ESEM in high-vacuum mode, at 5 keV. X-Ray photoelectron spectroscopy (XPS) is performed using a Kratos AXIS Ultra Imaging Spectrometer.

Resonant Raman spectroscopy [37] is performed using a Kaiser Hololab 5000R Raman Microprobe, with 514.5 nm (2.41 eV) Argon-Ion excitation (Coherent), and a 100 \times magnification objective focused to maximize the intensity of the Si signal. Spectra are taken with a single 15 s accumulation at each of five points per sample, and the individual spectra are shifted to match at the 521 cm^{-1} silicon peak and then averaged. The G/D peak intensity ratio is used as a rough measure of sample quality, because it is the relative response of graphitic carbon (at 1589 cm^{-1}) to defective carbon (at 1350 cm^{-1}) from intrinsic defects in the CNTs or amorphous carbon on the CNTs and the substrate. The G/Si ratio is an ordinal approximation of CNT yield. How-

ever, it must be cautioned that an increase in the quantity of CNTs both increases the G-band intensity and decreases the visibility of the substrate. The catalyst film and any amorphous deposits on the substrate decrease the Si signal. Furthermore, the relative intensity of the D-band peak increases and the Si peak decreases with higher magnification (smaller spot size). Therefore, it is imperative to use the same magnification and focus for examining each sample.

We verified film uniformity and process consistency among different samples taken from the same wafer and grown under identical conditions, giving 2- σ variation of $G/D = \pm 3.1$ and $G/Si = \pm 0.25$. Among individual samples taken from wafers from seven different depositions of the Mo/Fe/Al₂O₃ film, variation of $G/D = \pm 4.6$ and $G/Si = \pm 2.1$. For best consistency, the temperature and gas composition studies used samples taken from the same wafer.

3. Growth on flat silicon substrates

3.1. Study of growth temperature

To study the effect of temperature, otherwise identical experiments were conducted using 1 \times 1 cm samples of the Mo/Fe/Al₂O₃ film on Si, with 40/360 sccm H₂/CH₄, at temperatures ranging from 725 to 1025 °C. Fig. 1 shows SEM images of representative samples. No growth occurs at 725 °C, while from 750 to 900 °C a film of densely tangled small-diameter CNTs is grown. At 925 °C, a low density of CNTs protrudes from cracked clusters of large particles on the substrate, and CNTs rarely grow from the substrate areas in between the clusters. Because of the low density, we observe that these CNTs are individually at least several μm long, and are sometimes straight and suspended between neighboring clusters. At 1025 °C, soot forms in the furnace tube, likely due to the self-pyrolysis of CH₄. The soot particles, shown in Fig. 2, are approximately spherical with a diameter of 1 μm . Large-diameter fiber structures grow on the Mo/Fe/Al₂O₃ film at 1025 °C, and are also shown in Fig. 2.

The Raman spectra in Fig. 3 indicate that the films of Fig. 1 contain a large proportion of high-quality single-walled CNTs. This judgment is based on the position of the G-band peak near 1589 cm^{-1} , the high G/D ratio, and the presence of strong RBM peaks, and is confirmed by TEM examination. Several RBM peaks are observed on each sample in the range of 160–310 cm^{-1} , indicating SWNT diameters of approximately 0.8–1.6 nm. Fig. 4 plots the average G/D and G/Si ratios for each sample, confirming the observation from SEM imaging that the CNT yield reaches a sharp maximum at approximately 825 °C, and showing the quality is relatively constant at $G/D \cong 25$ for 775–875 °C. The variation in G/D

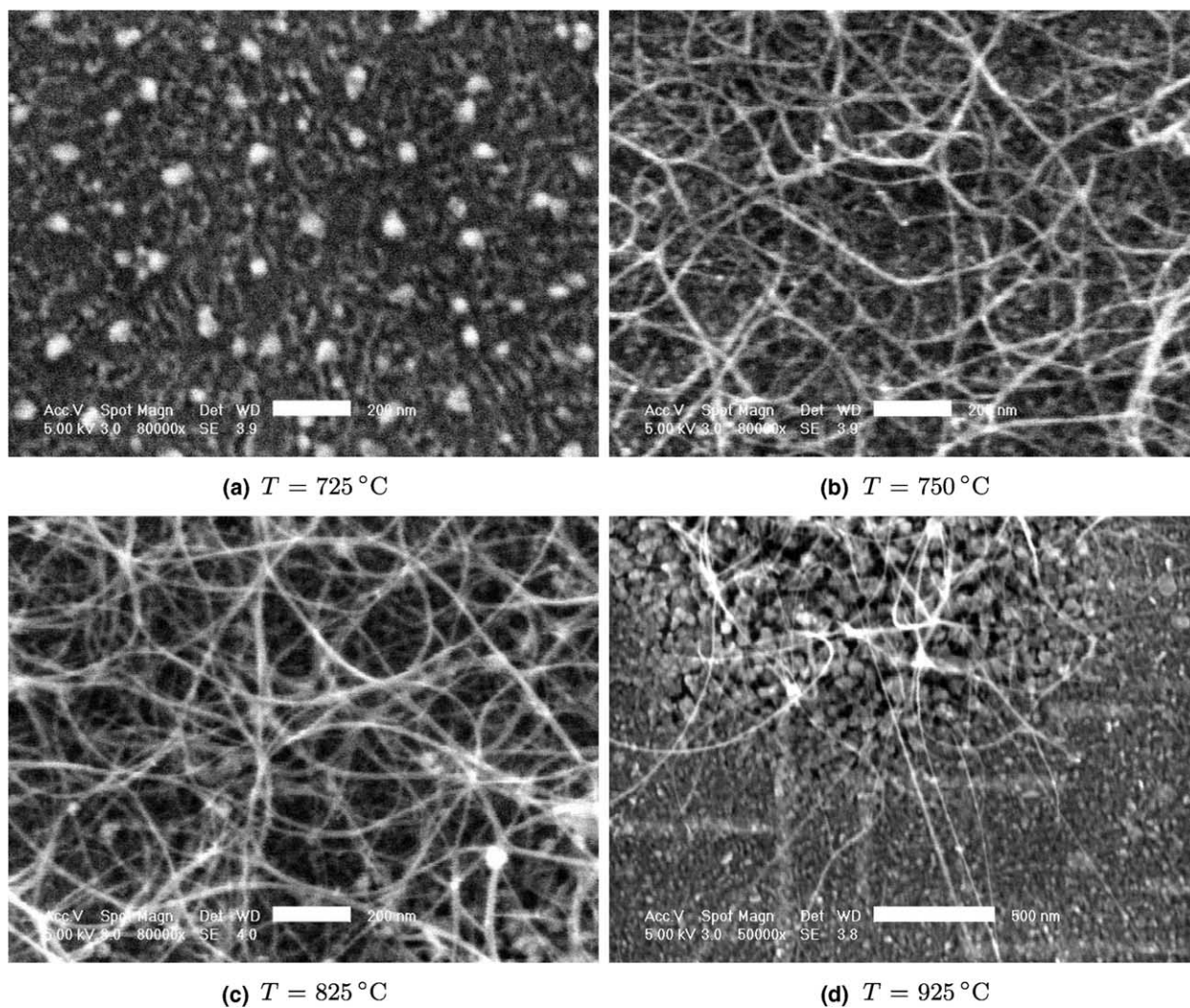


Fig. 1. SEM images of Mo/Fe/Al₂O₃ film processed in 400 sccm of 80:20 H₂/CH₄, at 725–925 °C. Scale is 200 nm on (a)–(c), and 500 nm on (d).

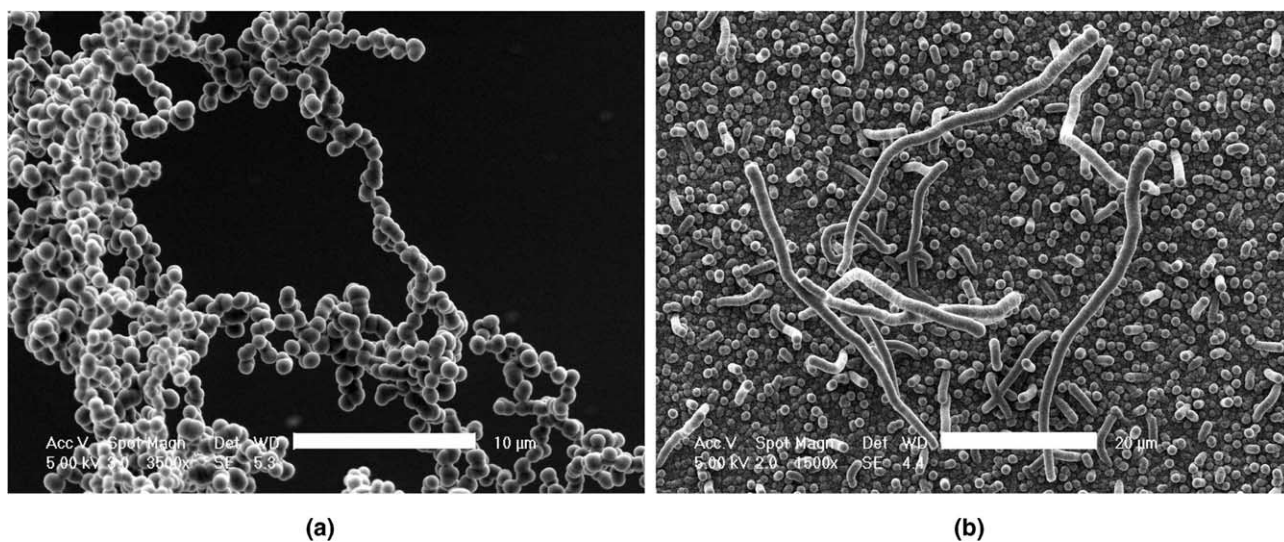


Fig. 2. Products formed at 1025 °C: (a) soot in furnace tube from pyrolysis of CH₄, scale 10 μm; (b) fibrous structures on Mo/Fe/Al₂O₃ film, scale 20 μm.

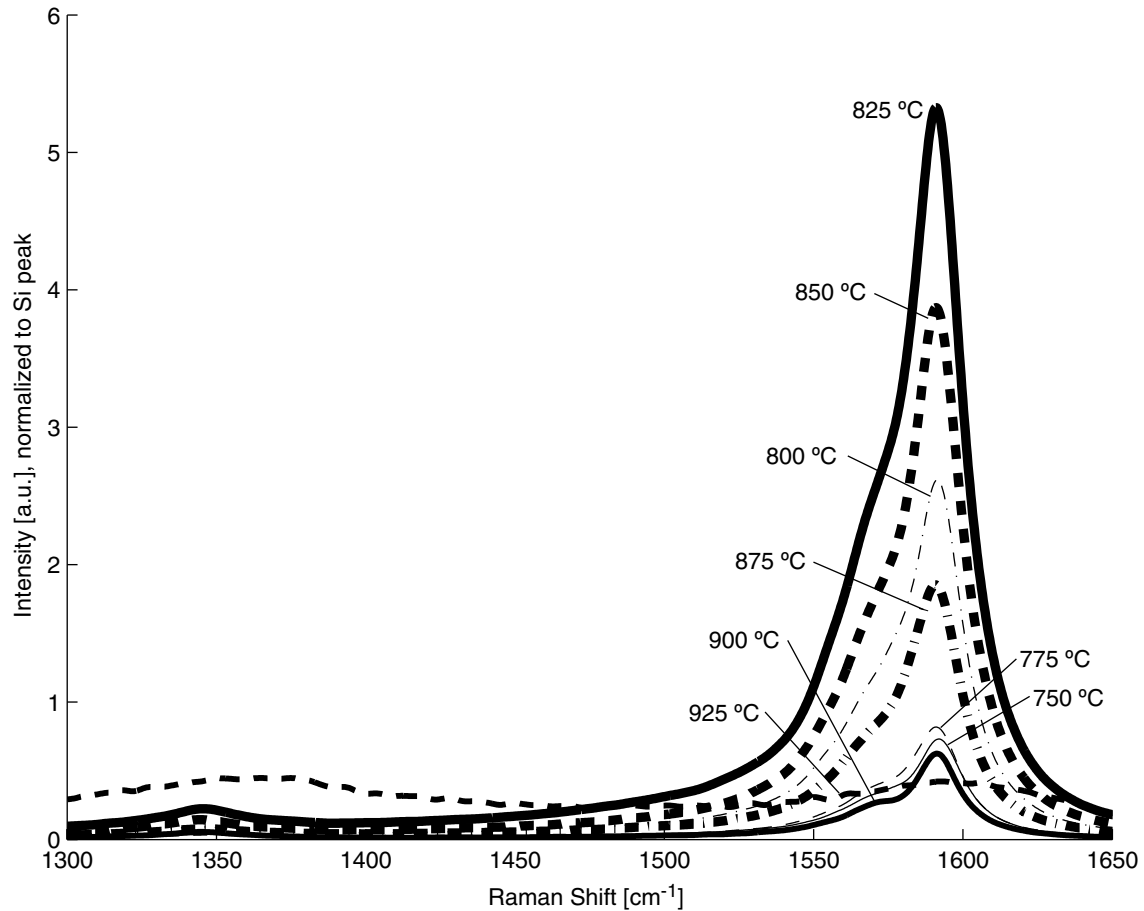


Fig. 3. G and D band regions of Raman spectra for samples with growth temperature of 750–925 °C, normalized to height of Si peak.

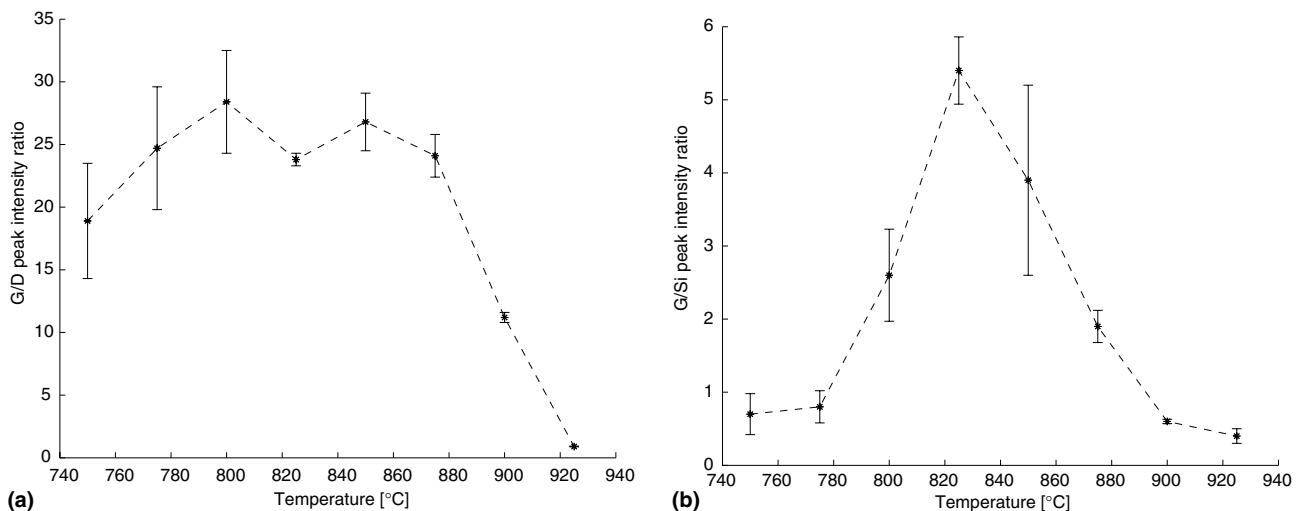


Fig. 4. Peak intensity ratios from Raman spectra (Fig. 3) of samples grown at 750–925 °C: (a) G/D ratio, indicating sample quality and (b) G/Si ratio, indicating sample yield.

and G/Si values from spectra taken at different points on the 825 °C sample is much less than samples grown at neighboring temperatures, demonstrating that this condition also gives a very uniform film texture.

3.2. Study of gas composition

To evaluate the effect of gas composition on CNT growth, otherwise identical experiments were conducted

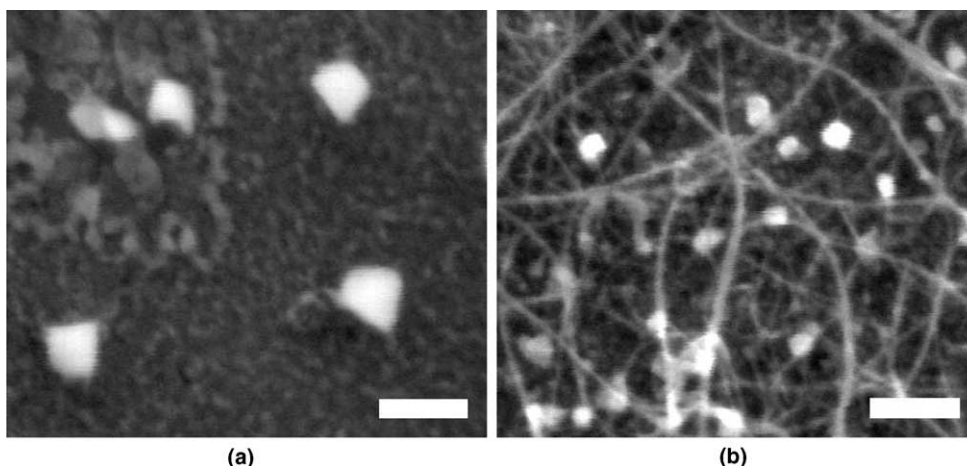


Fig. 5. Samples processed in 400 sccm of H_2/CH_4 at 875 °C, with (a) $H_2/CH_4 = 0.02$, insufficient for CNT growth and (b) $H_2/CH_4 = 0.09$, which gives highest yield. Scale 200 nm.

using 1×1 cm samples at 875 °C and a total flow of 400 sccm, varying the partial flows of H_2 and CH_4 . No CNT growth occurs from these samples in a pure CH_4 atmosphere, and CNT growth is first observed for $H_2/CH_4 \cong 0.04$. Fig. 5 shows SEM images of selected samples, and Fig. 6 shows the G/D and G/Si ratios from the Raman spectra. CNT yield rapidly reaches a maximum at $H_2/CH_4 \cong 0.09$, and is locally minimal at $H_2/CH_4 \cong 0.20$. Quality is first locally maximized between $H_2/CH_4 = 0.05$ and 0.07, then decreases as H_2 content increases, and then increases to a second maximum at $H_2/CH_4 \cong 0.20$. Although uncertainty in our data precludes a more certain conclusion, it appears that the maximum yield coincides with the first local minimum in quality, and that the local minimum of yield and maximum of quality at $H_2/CH_4 \cong 0.20$ are also coincident. An analogous behavior is observed on single long samples (1×10 cm) processed in pure CH_4 . On these samples, CH_4 is catalyzed into an evolving mixture containing H_2 and CH_4 as the gas flows along the surface of the sample, which causes the morphology, quality, and yield of CNTs to change significantly. These experiments will be discussed in a separate report.

3.3. Study of annealing and heating atmospheres

CNT growth from the Mo/Fe/ Al_2O_3 film is also affected significantly by “pre-baking” the catalyst sample, and by changing the atmosphere in which the catalyst is heated to the growth temperature. First, we consider a sample pre-baked in Ar for 30 min at 875 °C, subsequently cooled to room temperature, and then treated with the previously described (“normal”) Ar heating and H_2/CH_4 growth sequence. The G/Si ratio and the G/D ratio decrease 10–20% compared to a sample that was not pre-baked. When the catalyst is not pre-baked and is heated to the growth temperature in an atmosphere of 5% H_2 in Ar, no CNT growth occurs. How-

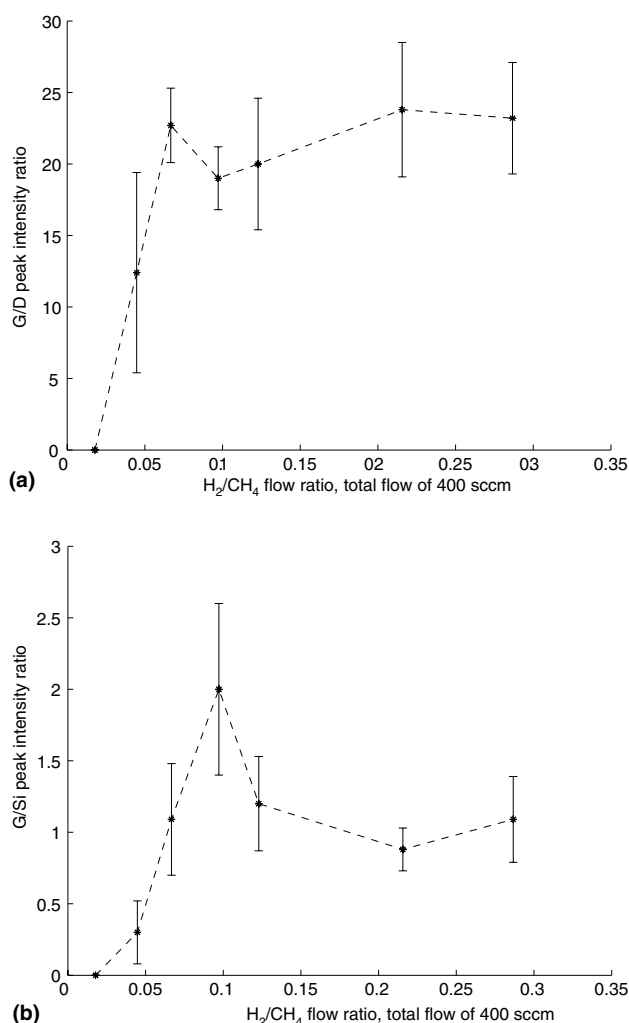


Fig. 6. Peak intensity ratios from Raman spectra of samples with processed in varying H_2/CH_4 environments: (a) G/D ratio and (b) G/Si ratio.

ever, when the sample is first pre-baked in Ar, cooled to room temperature, and then heated in 5% H_2/Ar

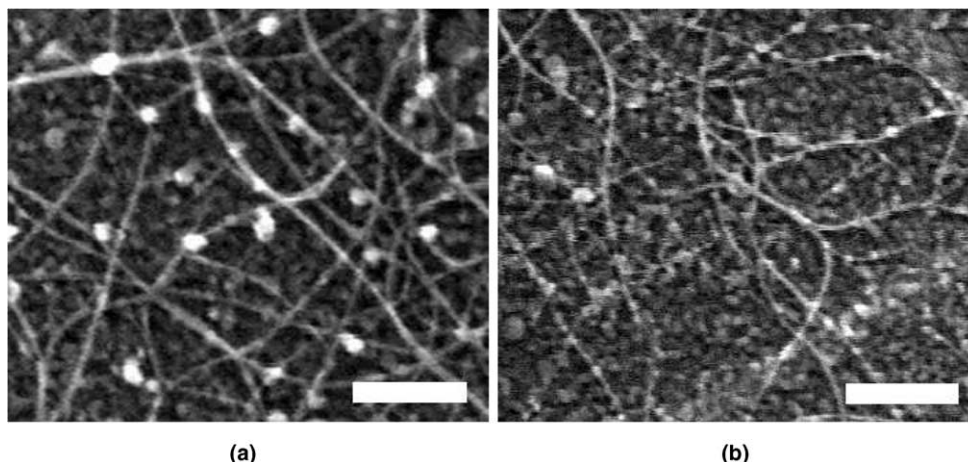


Fig. 7. Effects of annealing and heating: (a) sample annealed in Ar and heated in H_2/Ar and (b) sample annealed in H_2/Ar and heated in Ar. Scales 200 nm.

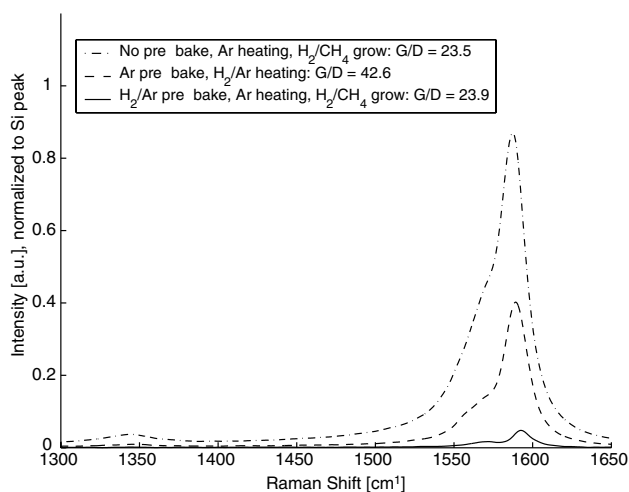


Fig. 8. Raman spectra of samples prebaked and heated in Ar and H_2/Ar atmospheres.

prior to the growth step, there is moderate CNT yield and the G/Si ratio is about 50% less than on a sample that was not pre-baked and was grown by the normal sequence (Figs. 7, 8). However, the G/D ratio is 80% higher than for the normal procedure without pre-baking, indicating a significant increase in CNT quality. When a sample is first treated in 5% H_2/Ar at 875 °C, cooled, and then processed normally, the CNT yield is very low, as confirmed by a sparse network of CNTs seen on the substrate and a G/Si ratio of only 0.05.

Ex situ XPS data shown in Fig. 9 indicates that the Mo layer in the Mo/Fe/ Al_2O_3 film is continuous as-deposited. This is apparent because only Mo(3p) and Mo(3d) peaks are seen in the spectrum of an as-deposited sample, while peaks for Al, Fe, and Mo appear in the spectrum of a sample annealed in Ar for 30 min at 875 °C. Angle-resolved XPS measurements, in which the penetration depth of the X-ray beam is varied by til-

ing the sample stage, show qualitatively how the chemical states of the elements change through the thickness of the film, due to interdiffusion upon annealing in Ar at 875 °C. The penetration depth is a maximum of 3–4 nm when the stage is horizontal (0° tilt), and decreases as the stage is tilted to the maximum angle of 70°. Fig. 9b shows that each element is more strongly oxidized near the surface of the film, because the peaks shift to higher binding energy as the stage tilt angle decreases [38]. The Al 2p spectrum shows the characteristic peak of Al at approximately 72 eV and Al_2O_3 at approximately 75 eV, and the relative strength of the Al_2O_3 peak increases at the surface. The doublet in the Fe 2p spectrum shows Fe_2O_3 ($2p_{3/2}$ at 711 eV and $2p_{1/2}$ at 725 eV), with a weak shift toward elemental Fe ($2p_{3/2}$ at 707 eV and $2p_{1/2}$ at 720 eV) as the penetration depth increases [39]. The Mo 3d signature suggests an increasing proportion of MoO_3 ($3d_{5/2}$ at 233 eV and $3d_{3/2}$ at 236 eV) near the surface, relative to Mo ($3d_{5/2}$ at 228 eV and $3d_{3/2}$ at 231 eV).

3.4. Discussion

The G/D ratio of our films, which is greater than 20 for most growth conditions, exceeds values previously reported for Fe and Mo/Fe catalysts supported on oxidized Al and spun-on Al_2O_3 films [23], indicating that the Al_2O_3 deposited by e-beam evaporation is especially effective as a supporting layer for CNT growth catalysts. Also, we suspect that Al_2O_3 directly promotes CNT growth, perhaps by feeding carbon to the catalyst particles by surface diffusion, as Al_2O_3 is known to catalyze the reorganization and decomposition of hydrocarbons at temperatures as low as 300 K [40]. Similar to the effect of adding H_2 to the gas mixture there may be an equilibrium effect of Al_2O_3 , and in general of the relative surface area of the oxide support. At one extreme, placing a large block of Al_2O_3 in the furnace tube

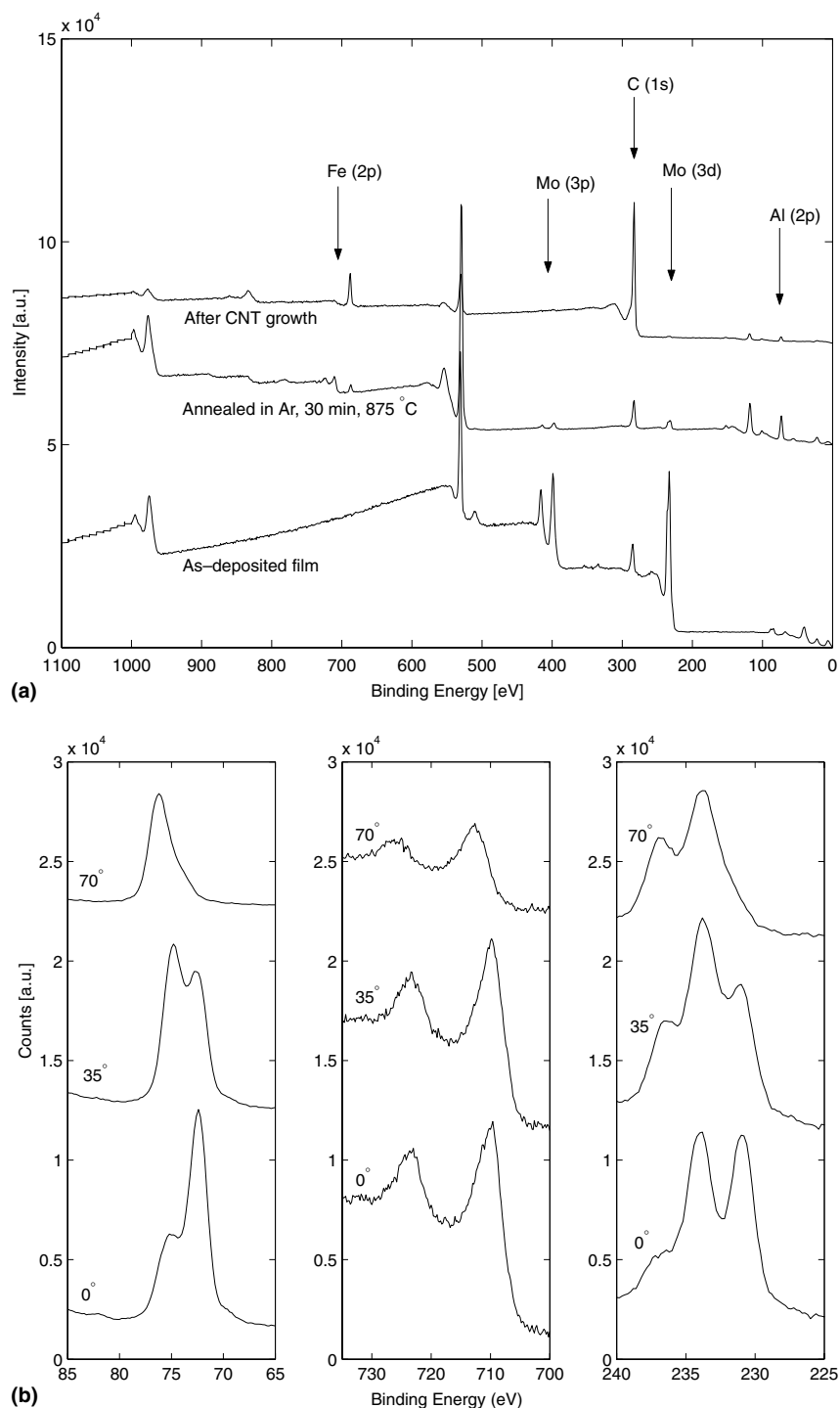


Fig. 9. Structure and composition of Mo/Fe/Al₂O₃ catalyst film, measured by X-Ray Photoelectron Spectroscopy (XPS): (a) comparison of as-deposited, annealed, and CNT samples and (b) through-thickness evolution of annealed sample, measured by angle-resolved XPS.

prevents CNT growth on a Mo/Fe/Al₂O₃ sample. Initially clean Al₂O₃ surfaces darken, indicating surface deposition of carbon, at conditions which otherwise do not cause self-pyrolysis of CH₄. At the other extreme, films of Mo/Fe on Si and SiO₂ show significantly lower yield than the Mo/Fe/Al₂O₃ film when processed under the same conditions.

It is well-known that treatment in H₂ enhances sintering of metal nanoparticles and promotes re-precipitation of metals from oxide supporting layers [41]; therefore, it is not unexpected that CNT growth is absent on a film heated in H₂/Ar without pre-baking. However, noting that all samples first pre-baked in Ar show at least moderate CNT yield, it appears that

high-temperature treatment in an oxidizing atmosphere stabilizes the film against the deleterious effects of H_2 . Numerous past results demonstrate there is a particle size “window” for CNT growth [16,42], where the carbon supply rate and activity must match the conditions for growth. When a thin film is heated, a broad distribution of particle sizes is created. This distribution is easily shifted by the annealing and heating atmosphere and process, but when the Fe/Mo catalyst remains oxidized prior to nucleation SWNT growth occurs over a broad range of processing conditions.

We also tested CNT growth from a 3.0/1.5/20 nm Mo/Fe/Al film on bare Si, as suggested by Ward et al. [23]. After heating in Ar, we were unable to grow CNTs, likely due to formation of an Al–Si eutectic at 577 °C, which deactivates the catalyst metal [26]. Growth after dedicated oxidation of the Al layer, by holding in air at 450 °C for 30 min prior to introduction of Ar and further heating to the growth temperature, yielded only a low density of poor-quality CNTs. We initially expected a higher CNT density because thin Al layers oxidize ra-

pidly in air [21]; however because the Mo top layer is continuous, it may slow oxidation of the Al until most of the Fe has diffused into the Al, giving a compound which is less effective for CNT growth.

Franklin et al. showed that CNT growth from a solution-prepared Mo/Fe/Al₂O₃ catalyst occurs in a narrow composition window of H_2/CH_4 spanning from approximately $H_2/CH_4 = 0.06–0.10$ [43]. They observed little or no yield from gas compositions outside this range; on one side there was an excess of active carbon species due to self-pyrolysis of CH_4 , and on the other side there was a deficit of active species. While the highest yield from our system falls within these limits, we further show high-activity from $H_2/CH_4 = 0.1–0.3$. It would be instructive to conduct experiments at a higher H_2/CH_4 ratio; however, at this stage, the configuration of our CVD apparatus limited our experiments to the range of flow compositions presented here.

Furthermore, we suspect that the interaction between Fe and Mo is qualitatively similar to that of the Co/Mo system, in which highly monodisperse clusters of Co are

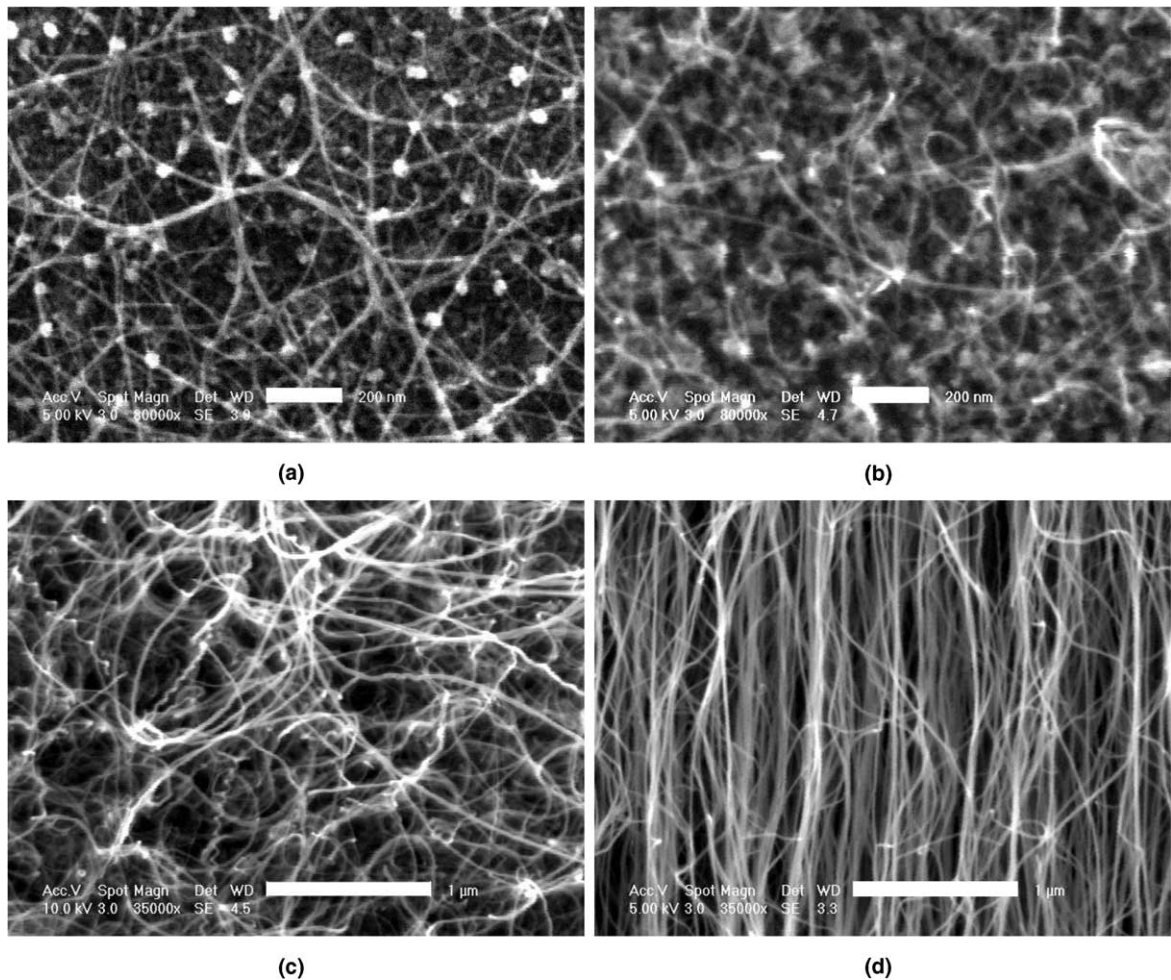


Fig. 10. Qualitative study of effect of Mo on CNT film growth: (a) Mo/Fe/Al₂O₃ in H_2/CH_4 , 875 °C (scale 200 nm); (b) Fe/Al₂O₃ in H_2/CH_4 , 875 °C (scale 200 nm); (c) Mo/Fe/Al₂O₃ in H_2/C_2H_4 , 750 °C (scale 1 μm) and (d) Fe/Al₂O₃ in H_2/C_2H_4 , 750 °C (scale 1 μm).

stabilized by an excess of Mo, giving a high-yield of SWNTs with a narrow diameter distribution [44,11]. Our catalyst has a definite excess of Mo (Mo/Fe = 2), and the excess Mo does not inhibit growth of SWNTs even though the solubility of Mo in Fe is only 7% and the total metal thickness of 5 nm likely produces metal clusters larger than the SWNT diameters we observed. It would be instructive to pursue a combinatorial approach to evaluate the effect of catalyst composition when there is an excess of Mo. A study spanning a range where Fe/Mo < 1, in which overlapping gradient films were deposited by pulsed laser deposition, demonstrated that Mo/Fe = 1/16 is the best ratio for growth of vertically-aligned MWNTs by thermal CVD of C₂H₂ [45].

Finally, to qualitatively evaluate the role of Mo and the hydrocarbon environment, we compared the performance of the Mo/Fe/Al₂O₃ film to a Fe/Al₂O₃ film, in H₂/CH₄ and in H₂/C₂H₄ environments. Fig. 10 shows SEM images of CNT growth from these four conditions. Versus the high-density SWNTs grown from Mo/Fe/

Al₂O₃, Fe/Al₂O₃ gives a much lower density of CNTs in H₂/CH₄. Mo/Fe/Al₂O₃ gives highly defective MWNTs in H₂/C₂H₄, whereas Fe/Al₂O₃ gives mm-high structures of vertically-aligned MWNTs. Therefore, Mo promotes growth of SWNTs from CH₄, but may retard the growth of MWNTs from C₂H₄. A complex interaction between Mo and Fe is further implied, because based on as-deposited thickness, we may expect the Fe film (1.5 nm) to give smaller particles than the Mo/Fe film (3.0/1.5 nm). We emphasize that the best parameters for CNT growth are tightly coupled for each catalyst and hydrocarbon environment; for example, the gas composition giving the highest yield changes with growth temperature, and the conditions for high-yield do not necessarily give the highest quality.

4. Growth on microstructured silicon substrates

Following the normal CVD procedure discussed previously, high-quality CNT films are also grown directly

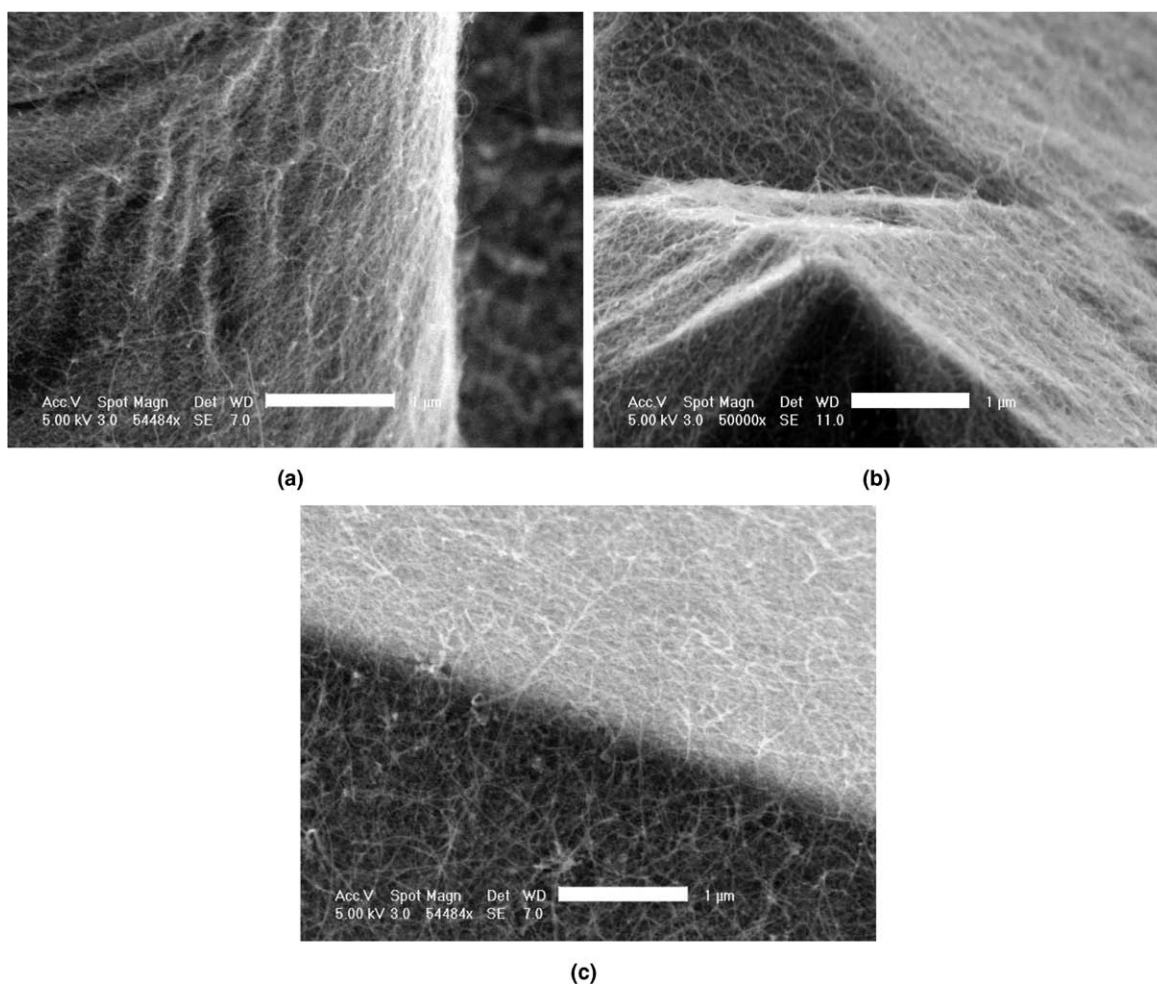


Fig. 11. CNT growth from Mo/Fe/Al₂O₃ catalyst on bulk-micromachined silicon microstructures: (a) film on vertical sidewall of cylindrical post fabricated by DRIE; (b) uniform film on pyramid inside KOH-etched microchannel and (c) transition between sidewall and floor of microchannel. Scales 1 μm.

and conformally on silicon microstructures. Bulk-micromachined structures are fabricated from (100) silicon wafers by deep-reactive ion etching (DRIE) using a $\text{SF}_6/\text{C}_4\text{F}_8$ plasma, by reactive ion etching (RIE) using a Cl_2 plasma, and by wet etching in aqueous KOH. The Mo/Fe/ Al_2O_3 catalyst film is deposited on the microstructures by the same process as for the flat silicon substrates; the wafer is placed horizontally and perpendicular to the evaporation source and during deposition the substrate holder is rotated in the horizontal plane. While the oblique microstructures, especially the vertical sidewalls of the DRIE-etched structures, expose smaller projected areas and therefore receive thinner metal layers than surfaces that directly face the evaporation source, we observe CNT growth on all topography, indicating that uniform scaling of the film thicknesses within a wide range does not significantly reduce the activity of the catalyst film. As expected, growth on the DRIE-etched vertical walls appears to be less dense than on the KOH-etched slanted surfaces; however, the moderate growth density on the vertical walls suggests that intermolecular collisions in the vapor flux direct a significant fraction of atoms to the sidewall surfaces.

Fig. 11 shows CNT films grown on a vertical sidewall etched by DRIE and a on pyramid structure within a microchannel etched in KOH. These films uniformly coat slanted surfaces (Fig. 11b) and make smooth transitions at corners (Fig. 11a and b). Suspended CNTs span distances of approximately 5 μm or less between nearby structures, such as across narrow V-grooves etched in KOH. Raman spectra are nearly identical on all horizontal and slanted silicon surfaces covered with CNTs, verifying film uniformity. However, the signals from SWNTs are often stronger when the spot is focused over a narrow trench, indicating resonance from suspended SWNTs.

5. Conclusion

We studied growth of high-quality CNT films on bare and microstructured silicon substrates by atmospheric pressure thermal CVD, from Mo/Fe/ Al_2O_3 deposited by e-beam evaporation. Dense SWNT growth occurs in gas mixtures containing at least 5% H_2 in CH_4 , at 750–900 °C. Presence of Mo and Al_2O_3 in addition to Fe promotes high-yield growth of SWNTs under these conditions. Comparatively, a Fe/ Al_2O_3 film gives vertically-aligned MWNTs in $\text{H}_2/\text{C}_2\text{H}_4$, but only a very low density of CNTs in H_2/CH_4 . These results reinforce the importance of synergy between the catalyst and gas activity in determining the morphology, yield, and quality of CNTs. Our methods are scalable to full-wafer areas, and conformal CNT film grown on bulk-micromachined structures encourages integration of CNT films as functional elements in micro devices.

Acknowledgements

This project was funded in part by an Ignition Grant from the MIT Deshpande Center for Technological Innovation. A.J. Hart is grateful for the support of a Fannie and John Hertz Foundation Fellowship. Thanks to Yet-Ming Chiang of the MIT Department of Materials Science and Engineering for use of his laboratory space, and the staffs of the MIT Microsystems Technology Laboratories and CMSE Shared Experimental Facilities (NSF DMR-0213282, #CHE-0111370) for assistance with fabrication and characterization. Further thanks to Jing Kong for her detailed review of the manuscript and to Teresa de los Arcos for her comments on the XPS analysis.

References

- [1] Snow ES, Novak JP, Campbell PM, Park D. Random networks of carbon nanotubes as an electronic material. *Appl Phys Lett* 2003;82(13):2145–7.
- [2] Star A, Han TR, Joshi V, Gabriel JCP, Gruner G. Nanoelectronic carbon dioxide sensors. *Adv Mater* 2004;16(22):2049–52.
- [3] Ghosh S, Sood AK, Kumar N. Carbon nanotube flow sensors. *Science* 2003;299(5609):1042–4.
- [4] Tzeng Y, Chen Y, Liu C. Electrical contacts between carbon-nanotube coated electrodes. *Diamond Relat Mater* 2003;12(3–7):774–9.
- [5] Meitl MA, Zhou YX, Gaur A, Jeon S, Usrey ML, Strano MS, et al. Solution casting and transfer printing single-walled carbon nanotube films. *Nano Letters* 2004;4(9):1643–7.
- [6] Qu SC, Fung CKM, Chan RHM, Li WJ. Development of an automated microinjection system for fabrication of carbon nanotube sensors. In: Fifth world congress on intelligent control and automation, Hangzhou, China, 2004, p. 5613–18.
- [7] Vander Wal RL, Ticich TM, Curtis VE. Substrate-support interactions in metal-catalyzed carbon nanofiber growth. *Carbon* 2001;39(15):2277–89.
- [8] Satterfield CN. Heterogeneous catalysis in industrial practice. 2nd ed. New York: McGraw-Hill; 1991.
- [9] Kong J, Soh HT, Cassell AM, Quate CF, Dai HJ. Synthesis of individual single-walled carbon nanotubes on patterned silicon wafers. *Nature* 1998;395(6705):878–81.
- [10] Lee CJ, Kim DW, Lee TJ, Choi YC, Park YS, Kim WS, et al. Synthesis of uniformly distributed carbon nanotubes on a large area of Si substrates by thermal chemical vapor deposition. *Appl Phys Lett* 1999;75(12):1721–3.
- [11] Resasco DE, Alvarez WE, Pompeo F, Balzano L, Herrera JE, Kitiyanan B, et al. A scalable process for production of single-walled carbon nanotubes (SWNTs) by catalytic disproportionation of CO on a solid catalyst. *J Nanopart Res* 2002;4(1–2):131–6.
- [12] Maruyama S, Miyauchi Y, Edamura T, Igarashi Y, Chiashi S, Murakami Y. Synthesis of single-walled carbon nanotubes with narrow diameter-distribution from fullerene. *Chem Phys Lett* 2003;375(5–6):553–9.
- [13] Shin YM, Jeong SY, Jeong HJ, Eum SJ, Yang CW, Park CY, et al. Influence of morphology of catalyst thin film on vertically aligned carbon nanotube growth. *J Cryst Growth* 2004;271(1–2):81–9.
- [14] Muller A, Das SK, Kogerler P, Bogge H, Schmidtman M, Trautwein AX, et al. A new type of supramolecular compound:

- molybdenum-oxide-based composites consisting of magnetic nanocapsules with encapsulated keggion-ion electron reservoirs cross-linked to a two-dimensional network. *Angewandte Chemie—International Edition* 2000;39(19):3414–7.
- [15] An L, Owens JM, McNeil LE, Liu J. Synthesis of nearly uniform single-walled carbon nanotubes using identical metal-containing molecular nanoclusters as catalysts. *J Am Chem Soc* 2002;124(46):13688–9.
- [16] Cheung CL, Kurtz A, Park H, Lieber CM. Diameter-controlled synthesis of carbon nanotubes. *J Phys Chem B* 2002;106(10):2429–33.
- [17] Choi GS, Cho YS, Son KH, Kim DJ. Mass production of carbon nanotubes using spin-coating of nanoparticles. *Microelectron Eng* 2003;66(1–4):77–82.
- [18] Murakami Y, Miyauchi Y, Chiashi S, Maruyama S. Direct synthesis of high-quality single-walled carbon nanotubes on silicon and quartz substrates. *Chem Phys Lett* 2003;377(1–2):49–54.
- [19] Kind H, Bonard JM, Emmenegger C, Nilsson LO, Hernadi K, Maillard-Schaller E, et al. Patterned films of nanotubes using microcontact printing of catalysts. *Adv Mater* 1999;11(15):1285–9.
- [20] Cassell AM, Franklin NR, Tomblor TW, Chan EM, Han J, Dai HJ. Directed growth of free-standing single-walled carbon nanotubes. *J Am Chem Soc* 1999;121(34):7975–6.
- [21] Jeurgens LPH, Sloof WG, Tichelaar FD, Mittemeijer EJ. Growth kinetics and mechanisms of aluminum-oxide films formed by thermal oxidation of aluminum. *J Appl Phys* 2002;92(3):1649–56.
- [22] de los Arcos T, Garnier MG, Oelhafen P, Mathys D, Seo JW, Domingo C, et al. Strong influence of buffer layer type on carbon nanotube characteristics. *Carbon* 2004;42(1):187–90.
- [23] Ward JW, Wei BQ, Ajayan PM. Substrate effects on the growth of carbon nanotubes by thermal decomposition of methane. *Chem Phys Lett* 2003;376(5–6):717–25.
- [24] Delzeit L, Chen B, Cassell A, Stevens R, Nguyen C, Meyyappan M. Multilayered metal catalysts for controlling the density of single-walled carbon nanotube growth. *Chem Phys Lett* 2001;348(5–6):368–74.
- [25] Lacerda RG, Teo KBK, Teh AS, Yang MH, Dalal SH, Jefferson DA, et al. Thin-film metal catalyst for the production of multi-wall and single-wall carbon nanotubes. *J Appl Phys* 2004;96(8):4456–62.
- [26] de los Arcos T, Wu ZM, Oelhafen P. Is aluminum a suitable buffer layer for carbon nanotube growth? *Chem Phys Lett* 2003;380(3–4):419–23.
- [27] Dai HJ, Rinzler AG, Nikolaev P, Thess A, Colbert DT, Smalley RE. Single-wall nanotubes produced by metal-catalyzed disproportionation of carbon monoxide. *Chem Phys Lett* 1996;260(3–4):471–5.
- [28] Deng WQ, Xu X, Goddard WA. A two-stage mechanism of bimetallic catalyzed growth of single-walled carbon nanotubes. *Nano Letters* 2004;4(12):2331–5.
- [29] Qi S, Yang B. Methane aromatization using Mo-based catalysts prepared by microwave heating. *Catal Today* 2004;98(4):639–45.
- [30] de los Arcos T, Garnier MG, Seo JW, Oelhafen P, Thommen V, Mathys D. The influence of catalyst chemical state and morphology on carbon nanotube growth. *J Phys Chem B* 2004;108(23):7728–34.
- [31] Kong J, Cassell AM, Dai HJ. Chemical vapor deposition of methane for single-walled carbon nanotubes. *Chem Phys Lett* 1998;292(4–6):567–74.
- [32] Dai HJ, Kong J, Zhou CW, Franklin N, Tomblor T, Cassell A, et al. Controlled chemical routes to nanotube architectures, physics, and devices. *J Phys Chem B* 1999;103(51):11246–55.
- [33] Seidel R, Duesberg GS, Unger E, Graham AP, Liebau M, Kreupl F. Chemical vapor deposition growth of single-walled carbon nanotubes at 600 °C and a simple growth model. *J Phys Chem B* 2004;108(6):1888–93.
- [34] Vasileva NA, Buyanov RA, Klimik IN. The catalytic pyrolysis of hydrocarbons. *Kinetics Catal* 1980;21(1):175–9.
- [35] Han IT, Kim BK, Kim HJ, Yang MH, Jin YW, Jung S, et al. Effect of Al and catalyst thicknesses on the growth of carbon nanotubes and application to gated field emitter arrays. *Chem Phys Lett* 2004;400(1–3):139–44.
- [36] Cao AY, Ajayan PM, Ramanath G, Baskaran R, Turner K. Silicon oxide thickness-dependent growth of carbon nanotubes. *Appl Phys Lett* 2004;84(1):109–11.
- [37] Jorio A, Pimenta MA, Souza AG, Saito R, Dresselhaus G, Dresselhaus MS. Characterizing carbon nanotube samples with resonance Raman scattering. *New J Phys* 2003;5:139.1–139.17.
- [38] Moulder JF, Chastain J. *Handbook of X-ray photoelectron spectroscopy: a reference book of standard spectra for identification and interpretation of XPS data*. Eden Prairie, MN: Perkin-Elmer Corporation; 1992.
- [39] Lin TC, Seshadri G, Kelber JA. A consistent method for quantitative XPS peak analysis of thin oxide films on clean polycrystalline iron surfaces. *Appl Surf Sci* 1997;119(1–2):83–92.
- [40] Knösinger H, Ratnasamy P. Catalytic aluminas. *Catal Rev* 1978;17:31–69.
- [41] Ago H, Nakamura K, Uehara N, Tsuji M. Roles of metal-support interaction in growth of single- and double-walled carbon nanotubes studied with diameter-controlled iron particles supported on mgo. *J Phys Chem B* 2004;108(49):18908–15.
- [42] Wong EW, Bronikowski MJ, Hoenk ME, Kowalczyk RS, Hunt BD. Submicron patterning of iron nanoparticle monolayers for carbon nanotube growth. *Chem Mater* 2005;17(2):237–41.
- [43] Franklin NR, Li YM, Chen RJ, Javey A, Dai HJ. Patterned growth of single-walled carbon nanotubes on full 4-inch wafers. *Appl Phys Lett* 2001;79(27):4571–3.
- [44] Alvarez WE, Kitiyanan B, Borgna A, Resasco DE. Synergism of Co and Mo in the catalytic production of single-wall carbon nanotubes by decomposition of CO. *Carbon* 2001;39(4):547–58.
- [45] Christen HM, Poretzky AA, Cui H, Belay K, Fleming PH, Geohegan DB, et al. Rapid growth of long, vertically aligned carbon nanotubes through efficient catalyst optimization using metal film gradients. *Nano Letters* 2004;4(10):1939–42.